



## **The DFNA5 gene, responsible for hearing loss and involved in cancer, encodes a novel apoptosis-inducing protein**

Ken Op de Beeck, Guy van Camp, Sofie Thys, Nathalie Cools, Isabelle Callebaut, Karen Vrijens, Luc van Nassauw, Viggo Fi van Tendeloo, Jean Pierre Timmermans, Lut van Laer

### **► To cite this version:**

Ken Op de Beeck, Guy van Camp, Sofie Thys, Nathalie Cools, Isabelle Callebaut, et al.. The DFNA5 gene, responsible for hearing loss and involved in cancer, encodes a novel apoptosis-inducing protein. European Journal of Human Genetics, 2011, 10.1038/ejhg.2011.63 . hal-00636188

**HAL Id: hal-00636188**

**<https://hal.science/hal-00636188>**

Submitted on 27 Oct 2011

**HAL** is a multi-disciplinary open access archive for the deposit and dissemination of scientific research documents, whether they are published or not. The documents may come from teaching and research institutions in France or abroad, or from public or private research centers.

L'archive ouverte pluridisciplinaire **HAL**, est destinée au dépôt et à la diffusion de documents scientifiques de niveau recherche, publiés ou non, émanant des établissements d'enseignement et de recherche français ou étrangers, des laboratoires publics ou privés.

**The *DFNA5* gene, responsible for hearing loss and involved in cancer, encodes a novel apoptosis-inducing protein**

Running title: ***DFNA5* encodes a novel apoptosis-inducing protein**

Ken Op de Beeck<sup>1</sup>, Guy Van Camp<sup>1,\*</sup>, Sofie Thys<sup>2</sup>, Nathalie Cools<sup>3</sup>, Isabelle Callebaut<sup>4</sup>, Karen Vrijens<sup>1</sup>, Luc Van Nassauw<sup>2,5</sup>, Viggo FI Van Tendeloo<sup>3</sup>, Jean Pierre Timmermans<sup>2</sup> and Lut Van Laer<sup>1</sup>

<sup>1</sup> Center of Medical Genetics, Department of Biomedical Sciences, University of Antwerp, 2610 Antwerp, Belgium

<sup>2</sup> Laboratory of Cell Biology & Histology, Department of Veterinary Sciences, University of Antwerp, 2020 Antwerp, Belgium

<sup>3</sup> Vaccine & Infectious Disease Institute (VIDI), Laboratory of Experimental Hematology, University of Antwerp, 2610 Antwerp, Belgium

<sup>4</sup> Department of Structural Biology, Institute of Mineralogy and Physics of Condensed Media, Université Pierre et Marie Curie-Paris6, Université Paris Diderot-Paris7, CNRS, 75015 Paris, France

<sup>5</sup> Laboratory of Human Anatomy & Embryology, Faculty of Medicine, University of Antwerp, 2020 Antwerp, Belgium

\* To whom correspondence should be addressed. Universiteitsplein 1, 2610 Wilrijk, Belgium

Tel: +323 275 97 62; fax: +323 275 97 22

e-mail: [guy.vancamp@ua.ac.be](mailto:guy.vancamp@ua.ac.be)

Key words : tumor suppressor, hearing loss, apoptosis, dfna5, cancer, hca, GSEA

## **Abstract**

*DFNA5* was first identified as a gene causing autosomal dominant hearing loss. Different mutations have been found, all exerting a highly specific gain of function effect, in which skipping of exon 8 causes the hearing loss. Later reports revealed the involvement of the gene in different types of cancer. Epigenetic silencing of *DFNA5* in a large percentage of gastric, colorectal and breast tumors and p53 dependent transcriptional activity have been reported, concluding that *DFNA5* acts as a tumor suppressor gene in different frequent types of cancer. Despite these data, the molecular function of *DFNA5* has not been investigated properly. Previous transfection studies with mutant *DFNA5* in yeast and in mammalian cells showed a toxic effect of the mutant protein which was not seen after transfection of the wild type protein. Here, we demonstrate that *DFNA5* is composed of two domains, separated by a hinge region. The first region induces apoptosis when transfected in HEK293T cells, the second region masks and probably regulates this apoptosis inducing capability. Moreover, the involvement of *DFNA5* in apoptosis related pathways in a physiological setting was demonstrated through gene expression microarray analysis using *Dfna5* knockout mice. In view of its important role in carcinogenesis, this finding is expected to lead to new insights on the role of apoptosis in many types of cancer. In addition, it provides a new line of evidence supporting an important role for apoptosis in monogenic and complex forms of hearing loss.

## **Introduction**

*DFNA5* first was discovered in a Dutch family with autosomal dominant hearing loss (HL) <sup>1</sup>. Not much was known concerning its cellular function and how its function was related to HL. Recently, a novel mutation in *DFNA5* has been identified in a Korean family, totaling 5 families with *DFNA5* hearing loss <sup>2</sup>. These families all have different genomic *DFNA5* mutations, but in each case the *DFNA5* mRNA transcript skips exon 8, resulting in a

1 frameshift and a premature truncation of the protein <sup>1-5</sup>. These findings have led to the  
2 hypothesis that *DFNA5* associated HL is attributable to a highly specific gain-of-function  
3 mutation, in which skipping of one exon causes disease while mutations in other parts of this  
4 gene may not result in HL at all. Further experimental evidence for this hypothesis was  
5 provided by the finding that transfection of mutant *DFNA5* causes cell death in both yeast <sup>6</sup>  
6 and mammalian <sup>7</sup> cells and by the discovery of a new *DFNA5* mutation <sup>8</sup>. The latter mutation  
7 truncated the protein in the fifth exon, but did not segregate with HL and was present in  
8 family members with normal hearing. The hypothesis was further corroborated by a mouse  
9 that lacked the *Dfna5* protein. This knockout (KO) mouse did not display any HL and, as a  
10 consequence, was not a suitable animal model to study *DFNA5* associated HL <sup>9</sup>.

11 To date, little information is available on the physiological function of *DFNA5*. However,  
12 since its identification, the small number of papers published on *DFNA5* almost all point to a  
13 possible involvement in cancer biology <sup>10-16</sup>. Especially during the last three years, *DFNA5*  
14 emerged from several genomic screens identifying new tumor suppressor genes. Further  
15 analysis showed that the *DFNA5* gene is epigenetically inactivated in several types of cancer,  
16 including gastric, colorectal and breast cancer <sup>13-16</sup>. Epigenetic silencing through methylation  
17 was found in 52 to 65% of primary tumors. In addition, *in vitro* studies showed that cell  
18 invasion, colony numbers, colony size and cell growth increased in cell lines after *DFNA5*  
19 knockdown. Forced expression of *DFNA5* in colorectal carcinoma cell lines, on the other  
20 hand, decreased cell growth and colony forming ability. In breast carcinoma, the methylation  
21 status of *DFNA5* was correlated with lymph node metastasis <sup>15</sup>. These recent data also explain  
22 earlier findings that were not well understood at the time, such as the increased resistance to  
23 the chemotherapeutic reagent etoposide in melanoma cells with decreased transcription of  
24 *DFNA5* <sup>11</sup>, or the finding that *DFNA5* is induced by p53 through a p53-binding site located in  
25 intron 1 <sup>12</sup>. of human acute lymphoblastic leukemia cell lines with the glucocorticoid

1 dexamethasone. This increase was only found in cells that underwent apoptosis in response to  
2 glucocorticoid treatment <sup>17</sup>. The conclusion of these data is that *DFNA5* is a tumor suppressor  
3 gene with an important role in several frequent forms of cancer.

4 Here we report that *DFNA5* contains two domains separated by a hinge region and that the  
5 first domain induces apoptosis when transfected into cell lines. The second domain may  
6 shield the apoptotic-inducing sequences residing in the first domain. Furthermore, using gene  
7 expression microarray experiments on *Dfna5* KO mice, we provide evidence that the  
8 apoptosis inducing properties of *DFNA5* also occur in a physiological setting and that  
9 *DFNA5* is involved in cell survival pathways.

## 10 **Materials and methods**

### 11 *Plasmid construction*

12 Using previously described human full-length *DFNA5* cDNA clones as a template <sup>6</sup>, we  
13 amplified full-length human wild type (WT) and mutant *DFNA5* sequences in addition to  
14 several specific parts of the *DFNA5* cDNA sequence using the iProof High Fidelity PCR kit  
15 (Bio-Rad Laboratories, Hercules, CA, USA) according to the manufacturer's instructions. A  
16 kozak consensus sequence (GCCACCATG) was introduced in the specific parts that lacked  
17 the regular *DFNA5* startcodon, either via PCR or via site-directed mutagenesis (Stratagene, La  
18 Jolla, CA, USA). PCR primers are listed in supplementary table I. All PCR fragments were  
19 ligated in pEGFP-N1. To clone the part of Pejvakin (*PJVK*) that showed high homology to  
20 *DFNA5*, human testis Quick-clone cDNA (BD Biosciences, San Jose, CA, USA) was used as  
21 a template. All cloned inserts were bidirectionally sequenced on an ABI 3730xl genetic  
22 analyzer (Applied Biosystems, Foster City, CA, USA).

### 23 *Transfection experiments*

24 HEK293T, HELA and MCF7 cells were subcultured in 60 mm dishes at a density of  $2 \times 10^5$   
25 cells in Dulbecco's modified Eagle's medium (DME) containing 4500 mg/l glucose

1 supplemented with 10% (volume/volume) fetal calf serum, 100 U/ml penicillin, 100 µg/ml  
2 streptomycin and 2 mM L-glutamine (all products from Invitrogen, San Diego, CA, USA).  
3 The cells were incubated overnight at 37°C in a 5% CO<sub>2</sub> humidified environment.  
4 Transfections were performed with a lipofectamine-plasmid emulsion as described previously  
5 <sup>7</sup>. 21 hours post transfection (16 hours for apoptosis assays; only for HEK293T cells), cells  
6 were harvested using TrypLE™ Express (Invitrogen) and diluted in 2 ml DME. Following  
7 centrifugation, the resulting cell pellet was resuspended in 500 µl D-PBS (Dulbecco's  
8 Phosphate-buffered Saline) (Invitrogen) and was subsequently used for flow cytometric  
9 evaluation.

#### 10 *Cell viability measurements*

11 Before measurements, 1 µl propidium iodide (PI) (1mg/ml) (Invitrogen) was added to the cell  
12 suspensions to enable discrimination between viable and dead cells. Cells were then evaluated  
13 on a FACScan flow cytometer (BD Biosciences). The gating strategy and cell counting was as  
14 described previously <sup>7</sup>. All measurements were independently replicated at least three times,  
15 unless stated otherwise. Cell viability was determined as the ratio of cells showing no PI  
16 fluorescence to the total cell population.

#### 17 *Confocal microscopy*

18 Cells for confocal microscopy were prepared as described previously <sup>7</sup>. Subcellular  
19 localization of selected constructs was performed using a Zeiss CLSM 510 confocal laser  
20 scanning microscope (Zeiss, Göttingen, Germany) equipped with an argon laser (excitation at  
21 488 nm) and two helium/neon lasers (excitation at 543nm and 630nm, respectively). To test  
22 whether the mutant *DFNA5* exon 9 – exon 10 construct was localised in the endoplasmic  
23 reticulum, double transfection with this construct and with pDsRed2-ER (Clontech) was  
24 performed in HEK293T cells. All images were taken at room temperature (RT) using a Zeiss  
25 C-Apochromat 63x/1.2 W Korr lens with Zeiss LSM 510 acquisition software.

### *Western Blotting*

HEK293T cells were subcultured at a density of  $4 \times 10^5$  cells per well and lipofected as described previously <sup>7</sup>. After 21 hours of incubation, cells were lysed on ice using RIPA buffer (150 mM NaCl, 50 mM Tris-HCL, 1% NP40, 0.5% Na-deoxycholate, 0.1% SDS), containing Complete Mini<sup>®</sup> protease inhibitors (Roche, Basel, Switzerland). The cell lysate was diluted in sample buffer (60 mM Tris-HCl, 50% glycerol, 2% SDS, 14.4 mM 2-mercaptoethanol, 0.1% Bromophenol Blue), heated for 5 minutes at 95°C, loaded on a 12% Tris-Glycine gel (Anamed, Gross-Bieberau, Germany) and electrophoretically separated. Next, the membrane was incubated with a primary rabbit anti-GFP antibody (1/2500) (Sigma, Missouri, USA) and a secondary goat anti rabbit-horse radish peroxidase-conjugated antibody (1/10000) (Sigma) afterwards. Subsequently, EGFP-fusion proteins were detected using Pierce ECL western blotting substrate (Thermo Scientific, Rockford, IL, USA).

### *Annexin V staining*

HEK293T cells were lipofected as described above. The standard harvesting time for the annexin V experiment was 16 hours post transfection. For the kinetic experiment harvesting times were: 3, 6, 9, 12, 16 and 24 hours post transfection. After harvesting, the cells were stained for annexin V using annexin V-biotin (Roche) according to the manufacturer's protocol. Before measurements, cells were stained with 1.3 µg/ml PI. Using a CyFlow ML cytometer (Partec, Görlitz, Germany), viable, early apoptotic, late apoptotic and necrotic cells were analyzed. Transfected annexin V-stained cells were also visualized using confocal microscopy.

### *TUNEL assay*

HEK293T cells were transfected as described above, harvested after 16 hours and a TUNEL assay ("in situ cell death detection kit", tetramethylrhodamine (TMR) red (Roche)) was performed according to the manufacturer's instructions. Cells were then resuspended in D-

1 PBS (Invitrogen), cytopinned and enclosed in Citifluor (Ted Pella, Redding, CA, USA).  
2 Cytospins were studied using confocal microscopy. Random images were taken at RT with  
3 Zeiss LSM 510 acquisition software on a Zeiss CLSM510 Meta microscope using a Zeiss C-  
4 Appochromat 40x/1.2 W Korr lens. For each experiment, the total number of TUNEL positive  
5 cells and the total number of cells were counted from 10 random images, using the AnalySIS  
6 software.

7 *Microarray expression analysis of Dfna5 KO versus WT mice and subsequent real time PCR*  
8 *verification*

9 Inner ear samples were removed from 9 WT (+/+) postnatal day 0 (P0) and 9 *Dfna5* KO (-/-)  
10 (P0) C57Bl/6J mice and mechanically homogenized, after which total RNA was extracted  
11 using the RNeasy kit (Qiagen, Hilden, Germany) according to the manufacturer's instructions.  
12 RNA quality was verified using the Experion system (Biorad). Subsequently, 9 RNA samples  
13 from WT mice were pooled in 3 WT RNA pools and 9 RNA samples from KO mice were  
14 pooled in 3 KO RNA pools. RNA pools were labeled with either Cy3 or Cy5 dyes, and  
15 hybridized on a Whole Mouse Genome Array (41K array) (Agilent, Santa Clara, CA, USA).  
16 Each experiment was followed by a colourflip, resulting in a total of 6 microarray  
17 experiments. The resulting intensity data was analyzed using the R-package "limma" (v3.2.1)  
18 and the Gene Set Enrichment Analysis (GSEA) program (v2.0, Broad Institute)<sup>18</sup>. Gene sets  
19 for GSEA were downloaded from the Gene Ontology (GO) website  
20 (<http://www.geneontology.org/>). These microarray results were validated with real time PCR  
21 using the RNA pools from the microarray experiment and a one step Power SYBR green PCR  
22 master mix (Applied Biosystems) according to the manufacturer's instructions on a  
23 Lightcycler 480 instrument (Roche). The resulting gene expression data were analyzed using  
24 Qbase plus (Biogazelle, Gent, Belgium) software.

25 *Statistical Analysis*



1 All statistical analyses were performed using one-way ANOVA. P values below 0.05 were  
2 considered statistically significant. Statistics were calculated using SPSS 15.0 (SPSS inc,  
3 Chicago, IL, USA)

#### 4 **Results**

##### 5 Gross mapping of the toxic region

6 All *DFNA5* mutations that cause hearing loss lead to exon 8 skipping. Therefore, we tested  
7 whether the toxicity of the mutant protein was due to the aberrant tail of 41 amino acids (AA)  
8 that is present in the mutant protein, as the first seven exons are identical in WT and mutant  
9 *DFNA5*<sup>7</sup>. We cloned the first part of *DFNA5* (exon 2 – exon 7) and generated three constructs  
10 based on the second part of *DFNA5* (exon 8 – exon 10 and exon 9 – exon 10 in the WT as  
11 well as in the mutant reading frame (figure 1A)) in a pEGFP-N1 vector. The expression of the  
12 fusion proteins was confirmed by western blotting (figure 1B). Figure 1C clearly  
13 demonstrates that transfection of the first part of *DFNA5* in HEK293T cells causes a  
14 significant drop in cell viability when compared to transfection of WT *DFNA5* (p<0.001).  
15 This was an interesting finding because this part of the protein is shared by WT and mutant  
16 protein. None of the constructs of the second part of *DFNA5* induced cytotoxicity.

17 The C-terminal part of *DFNA5* does not have an inhibitory effect on the cytotoxicity  
18 displayed by the N-terminal part of *DFNA5*, as the viability after double transfections with  
19 the WT *DFNA5* exon 2 – exon 7 and the WT *DFNA5* exon 9 - exon 10 construct or with the  
20 WT *DFNA5* exon 2 – exon 6 and the WT *DFNA5* exon 8 – exon 10 construct was comparable  
21 to that observed when transfecting the WT *DFNA5* exon 2 - exon 7 construct alone (results  
22 not shown).

23 The subcellular localization of these EGFP-tagged proteins was determined (figure 1D).  
24 Transfection of the WT *DFNA5* exon 2 – exon 7 construct resulted in a fusion protein that  
25 was expressed mainly at the plasma membrane. In addition, it was observed in the cytoplasm

1 in a granulated manner. The majority of cells transfected with this construct showed an  
2 unhealthy appearance (*i.e.*, cell blebbing). Overall, the expression pattern was very similar to  
3 that of mutant DFNA5<sup>7</sup>. WT DFNA5 exon 8 – exon 10 and WT DFNA5 exon 9 – exon 10  
4 exhibited a highly similar expression pattern. Both fusion proteins were distributed along the  
5 cytoplasm and cluster near the nucleus. Finally, cells transfected with mutant *DFNA5* exon 9  
6 – exon 10 showed EGFP expression primarily in the endoplasmic reticulum (ER). This was  
7 confirmed by cotransfection experiments with pDsRed2-ER, in which the EGFP signal of  
8 mutant *DFNA5* exon 9 – exon 10 colocalized with the signal of DsRed (supplementary figure  
9 1).

#### 10 Hydrophobic Cluster Analysis (HCA)

11 Simultaneously with the experiments described above, the sequence of DFNA5 was analyzed  
12 through HCA and compared to those of the DFNA5-gasdermin family, to which DFNA5  
13 belongs (figure 2). This technique of protein sequence analysis allows the simultaneous  
14 comparison of primary and secondary structures<sup>19-21</sup>.

15 From the comparison of DFNA5-gasdermin family members, DFNA5 can be divided in three  
16 distinct domains: a globular domain A (exon 2 – exon 6), a hinge region (exon 6 – exon 7)  
17 which is variable in length and sequence among the different DFNA5-gasdermin members  
18 and a globular domain B (exon 7 – exon 10). Domain A, which is common to all members of  
19 the DFNA5-gasdermin family, had an  $\alpha/\beta$  fold, whereas domain B, which is present in  
20 GSDM1 and MLZE but not in PJVK (in this case, it is replaced by a zinc-finger domain), had  
21 an all  $\alpha$  fold (mainly  $\alpha$ -helical structures). The lengths and shapes of the hydrophobic clusters  
22 within domain B suggested the presence of long helical structures, which might form coiled-  
23 coils.

24 Based on the division proposed by HCA, we constructed two plasmids, the first one  
25 containing HCA part A and the second HCA part B. When transfected in HEK293T cells,

1 domain A but not domain B was able to induce a toxic effect when compared to WT DFNA5  
2 (see supplementary table II). This finding enabled us to exclude exon 7 as part of the toxic  
3 region since this exon was not present in domain A of DFNA5.

4 Domain A of DFNA5 is highly similar to the first part of PJVK. To investigate whether the  
5 mechanism of toxicity was a conserved feature among the two members of the DFNA5  
6 family, we cloned the first part of *PJVK* (as indicated by HCA) in the pEGFP-N1 vector.  
7 After overexpression of the first part of *PJVK* in HEK293T cells, we measured no viability  
8 drop (see supplementary table II).

#### 9 Further delineation of the toxic region

10 The toxic region of DFNA5 was further delineated through the generation of different  
11 constructs. In a first series of constructs, *DFNA5* was truncated exon per exon starting from  
12 exon 7 towards the N-terminal region (supplementary figure 2). In another series of constructs  
13 *DFNA5* was truncated exon per exon from the N-terminal region towards exon 7  
14 (supplementary figure 3). The conclusion of these series of experiments was that an essential  
15 part of the toxic DFNA5 region was located somewhere in exon 6 and that the presence of  
16 exon 2 was essential for the toxic effect.

17 The toxic motif did not consist of a single exon as was demonstrated by the transfection of  
18 *DFNA5* exons 2 to 7 separately (see supplementary table II). In addition, transfection of  
19 constructs similar to WT DFNA5 HCA domain A, but lacking specific exons (either lacking  
20 exon 3, exon 4 or exon 5) did not lead to a detectable viability loss (see supplementary table  
21 II), indicating that the complete region between exon 2 and 6 is required for correct folding of  
22 the toxic domain.

#### 23 Cell Death evaluation.

24 The fate of cells transfected with mutant *DFNA5* was investigated using two independent  
25 assays: annexin V staining and TUNEL labeling.

## 1 *Annexin V staining*

2 To distinguish between apoptotic and necrotic cells, we performed a double labeling, using  
3 annexin V and PI. Early apoptotic cells were positive for annexin V, but not for PI. Late  
4 apoptotic cells were positive for both annexin V and PI (due to secondary necrosis), while  
5 necrotic cells emitted fluorescent signals only from PI.

6 Cells were transfected with an empty EGFP vector and with WT and mutant *DFNA5*-EGFP  
7 constructs and were visualized using confocal laser microscopy (figure 3A). The vast majority  
8 of cells transfected with WT *DFNA5*, showed no signs of PI or annexin V staining, while cells  
9 transfected with mutant *DFNA5* exhibited clear annexin V-Cy5 staining at their plasma  
10 membranes. Since no PI staining could be detected, this finding clearly indicated that cell  
11 death caused by mutant *DFNA5* was due to an apoptotic process.

12 To obtain quantitative results, we stained transfected HEK293T cell suspensions with annexin  
13 V-Cy5. Prior to flow cytometric analysis we also added PI to the cell suspensions. This  
14 allowed to discriminate between the viable, early apoptotic, late apoptotic and necrotic  
15 fractions. A typical flow cytometric result is shown in supplementary figure 4. To obtain the  
16 total apoptotic fraction in each cell suspension, we added the early apoptotic to the late  
17 apoptotic fraction. The bar charts in figure 3B summarize the average total apoptotic fraction  
18 (3 independent measurements) for each transfected cell suspension. Cells transfected with  
19 mutant *DFNA5* had a higher total apoptotic fraction ( $31.87\% \pm 7.82$ ) than cells transfected with  
20 WT *DFNA5* ( $18.32\% \pm 5.51$ ). Although the difference between the two groups was not  
21 statistically significant ( $p=0.07$ ), the trend was clearly visible.

## 22 *TUNEL Assay*

23 We transfected HEK293T cells with WT *DFNA5* and mutant *DFNA5*-EGFP constructs and an  
24 empty EGFP vector as negative control. Further controls included an untransfected and a  
25 mock transfected cell population. After staining, we counted the average TUNEL-positive

1 cells in 10 randomly captured images and made a ratio of these positive cells to the total  
2 number of cells present in these images (figure 4). A statistically significant difference  
3 ( $p=0.02$ ) was observed between mutant *DFNA5* transfected cells and cells transfected with  
4 WT *DFNA5*. The combined results of TUNEL and annexin V staining clearly indicate that  
5 toxicity induced by mutant *DFNA5* was due to apoptosis.

#### 6 *Microarray experiments using WT and Dfna5 KO mice*

7 To evaluate whether the apoptosis inducing features of *DFNA5* could also be demonstrated in  
8 a physiological setting, we performed a microarray gene expression analysis on WT and  
9 *Dfna5* KO mice using the Agilent Whole Mouse Genome Array (41k). Differential gene  
10 expression was estimated and 92 genes were statistically significant upregulated (adjusted  $p$   
11 value less than 0.05) in KO mice, while 88 genes were statistically significant downregulated  
12 in KO mice when compared to WT mice. From this list, four genes were selected and their  
13 expression patterns were evaluated using real time PCR and compared to those obtained from  
14 the microarray study. The differential expression of these genes was very similar between the  
15 two techniques (supplementary figure 5 and supplementary table III), indicating that the  
16 microarray results were reliable. Next, a gene set enrichment analysis (GSEA) was performed  
17 to check whether specific biological pathways were up- or downregulated in these mice to  
18 extract biologically meaningful conclusions. The analysis revealed 73 upregulated gene sets  
19 and 225 downregulated gene sets in KO mice (pathways with a False Discovery Rate (FDR) <  
20 25%; see supplementary table IV and V for a list of these pathways). Particularly, gene sets  
21 involved in cartilage maintenance (indicated in red in supplementary table IV) and DNA  
22 repair (indicated in blue in supplementary table IV) are upregulated in *Dfna5* KO mice, while  
23 gene sets involved in energy metabolism (indicated in orange in supplementary table V) and  
24 apoptosis (indicated in purple in supplementary table V) are downregulated in *Dfna5* KO  
25 mice.

## 1 **Discussion**

2 In the current study, we showed that induction of apoptosis is an intrinsic feature of the  
3 physiological function of DFNA5. We previously assumed that transfection of mutant *DFNA5*  
4 causes necrotic cell death <sup>7</sup>. Since increasing evidence of tumor suppressor gene  
5 characteristics of DFNA5 has been provided <sup>11,12,14</sup>, we re-evaluated the nature of mutant  
6 DFNA5-induced cell death. In this report, we used annexin V as well as TUNEL staining.  
7 Both techniques showed that transfection of mutant *DFNA5* resulted in cell death due to  
8 apoptosis. A likely explanation for the misinterpretation <sup>7</sup> may be that the time-lapse between  
9 transfection and assaying for cell death was too long in our previous report. We previously  
10 waited 24 hours before harvesting the cells <sup>7</sup>, versus 16 hours in the current study. We further  
11 investigated this concept with an experiment to establish the kinetics of mutant DFNA5-  
12 induced cell death. In a kinetic experiment, we harvested cells transfected with WT and  
13 mutant *DFNA5* after 3, 6, 9, 12, 16 and 24 hours (results not shown). Apoptotic events,  
14 identified as a positive signal for annexin V staining, became evident as soon as 6 hours after  
15 transfection with mutant *DFNA5*, and remained evident up to the time point of 16 hours, our  
16 standard harvesting time. Cells that were harvested after 24 hours had already shifted from  
17 late apoptotic cell death to secondary necrotic cell death.

18 In this study, we localized two essential sections of the apoptosis-inducing domain. Our  
19 results demonstrate that the apoptosis-inducing domain is not merely a linear domain located  
20 in a single or a few exons, but a three-dimensional structure consisting of different non-  
21 contiguous parts of the protein, and that the complete region between exon 2 and exon 6 may  
22 be critical for the correct formation of the apoptosis-inducing motif. This implicates that  
23 proper folding of the globular domain formed by the region including exon 2 to exon 6 is  
24 essential.

1 The apoptosis-inducing mechanism of DFNA5 is not limited to transfections of HEK293T  
2 cells. Previously, we showed that transfection of mutant *DFNA5* results in a viability loss in  
3 COS cells <sup>7</sup>. Here, we extended our analysis and transfected additional cell lines (MCF7 and  
4 HELA) with mutant and WT *DFNA5* (see supplementary figure 6). It appeared that  
5 transfection efficiencies in these cell lines were much lower than those obtained in HEK293T.  
6 Hence, transfection of mutant *DFNA5* did not impact viability of the overall cell population.  
7 However, when only GFP positive subpopulations were taken into account, it was clear that  
8 mutant *DFNA5* causes a significant drop in viability which is not seen after transfection of  
9 WT *DFNA5*. In conclusion, the apoptosis inducing mechanism of DFNA5 is not limited to  
10 transfections in HEK293T, but is present in all investigated cell lines so far.

11 Gene expression microarray experiments on WT and *Dfna5* KO mice, followed by pathway  
12 analysis revealed that apoptosis inducing pathways are downregulated in *Dfna5* KO mice. As  
13 such, we provide the first experimental evidence that the apoptotic features of DFNA5 are not  
14 only limited to overexpression experiments, but are also present in a physiological setting.  
15 Additionally, we have observed an upregulation of the DNA repair mechanisms in *Dfna5* KO  
16 mice. The latter could be explained by the fact that when apoptotic pathways are  
17 downregulated, DNA repair mechanisms need to be upregulated to maintain viable  
18 conditions.

19 Interestingly, genes involved in cartilage maintenance were also upregulated in *Dfna5* KO  
20 mice, linking our findings to those obtained by Busch-Nentwich et al.<sup>22</sup>. They found that  
21 zebrafish injected with *Dfna5* morpholino's displayed an absent expression of *Ugdh*, (UDP-  
22 glucose dehydrogenase) leading to reduced production of hyaluronic acid resulting in  
23 impaired facial cartilage differentiation. As *Dfna5* KO mice do not display this phenotype, it  
24 is possible that the gene sets involved in cartilage development provide compensatory  
25 mechanisms resulting in the lack of phenotype in these mice.

1 DFNA5 and PJVK clearly form a separate group within the DFNA5-gasdermin family <sup>23</sup>,  
2 while the other group includes GSDM1, MLZE and homologues. Although the two families  
3 evolved from a common ancestor, phylogenetic analysis has indicated that the two clades are  
4 distinct <sup>24</sup>, leaving DFNA5 with only a single closely related protein: PJVK. The first part of  
5 PJVK shows high similarity with DFNA5, but does not induce apoptosis. This is a first  
6 indication that the apoptosis-inducing mechanism may be specific for DFNA5 and that it may  
7 not be a general feature of the DFNA5 protein family.

8 Still, some questions remain to be clarified. Given the finding that the apoptosis-inducing  
9 domain is present in both WT and mutant DFNA5, the question arises as to why transfections  
10 with WT *DFNA5* did not result in cell death. A plausible explanation could be that the last  
11 part of the protein may quench or shield the part in which the apoptosis-inducing domain  
12 resides, so that apoptosis is not expressed in normal cellular conditions. Because the mutation  
13 changes and shortens the last part of the protein (starting from exon 8), the shielding function  
14 of this part of the protein may be neutralized and, as a consequence, apoptosis may be  
15 unleashed. This remains to be further investigated, for example by the resolution of the crystal  
16 three-dimensional structure of DFNA5.

17 Methylation of the 5'-flanking region of *DFNA5*, as frequently observed in gastric, colorectal  
18 and breast carcinoma <sup>13-16</sup> may be a way to prevent the apoptotic actions of DFNA5. We  
19 believe that our description of the apoptosis-inducing mechanism of DFNA5 contributes to  
20 the growing evidence that *DFNA5* may be a tumor suppressor gene. As apoptosis induction  
21 seems to be an intrinsic feature of DFNA5's function, it is likely that the WT DFNA5 protein  
22 can be activated to induce apoptosis in the cell under certain conditions. The nature of this  
23 regulating mechanism however, remains to be elucidated.

24 DFNA5-associated hearing loss is nonsyndromic and has so far not been associated with other  
25 symptoms. Still, *DFNA5* is present in every tissue investigated so far, albeit at low levels of



1 expression. In our opinion, it is unlikely that massive apoptotic cell death takes place in  
2 cochleae of *DFNA5* mutation carriers, or in any of the other tissues where *DFNA5* is  
3 expressed. A more plausible scenario for the *in vivo* situation is that expression of mutant  
4 *DFNA5* is a pro-apoptotic factor in the cell and that especially terminally differentiated cells,  
5 such as cochlear hair cells, are vulnerable to mutant *DFNA5*-induced programmed cell death.  
6 This cochlear hair cell loss may then be manifested as hearing loss. The fact that *DFNA5*-  
7 associated hearing loss is progressive in nature, seems compatible with this hypothesis. The  
8 role of apoptosis in cochlear cells resulting in auditory pathology has been described  
9 previously. For example, it has been demonstrated that apoptosis occurs in outer hair cells in  
10 mice displaying age related hearing loss <sup>25</sup>. Recently, a report was published implicating  
11 apoptosis in monogenic hearing loss. Overexpression of *TJP2* leads to altered expression of  
12 apoptosis related genes, ultimately causing hearing loss <sup>26</sup>. We believe that our study  
13 provides a new line of evidence supporting an important role of apoptosis in hearing loss.  
14 In conclusion, we have demonstrated that *DFNA5* is an apoptosis-inducing protein. In  
15 addition, it becomes increasingly clear that *DFNA5* not only functions in the auditory  
16 pathway, but is probably also implicated in a more fundamental role involving cell survival  
17 and apoptosis.

#### 18 **Conflict of interest**

19 The authors declare no conflict of interest.  
20

#### 21 **Acknowledgements**

22 This work was supported by grants of the European Community (Eurohear) and the ‘Fonds  
23 voor Wetenschappelijk Onderzoek Vlaanderen’ (FWO grant G.0245.10N). K.O.D.B. holds a  
24 predoctoral research position with the ‘Instituut voor de Aanmoediging van Innovatie door  
25 Wetenschap en Technologie in Vlaanderen (IWT)’.

Supplementary information is available at the European Journal of Human Genetics's website.

### **References**

1. Van Laer L, Huizing EH, Verstreken M *et al*: Nonsyndromic hearing impairment is associated with a mutation in DFNA5. *Nat Genet* 1998; **20**: 194-197.
2. Park HJ, Cho HJ, Baek JI *et al*: Evidence for a founder mutation causing DFNA5 hearing loss in East Asians. *Journal of Human Genetics* 2009.
3. Cheng J, Han DY, Dai P *et al*: A novel DFNA5 mutation, IVS8+4 A>G, in the splice donor site of intron 8 causes late-onset non-syndromic hearing loss in a Chinese family. *Clin Genet* 2007; **72**: 471-477.
4. Bischoff AMLC, Luijendijk MWJ, Huygen PLM *et al*: A second mutation identified in the DFNA5 gene in a Dutch family. A clinical and genetic evaluation. *Audiol Neuro-otol* 2004; **9**: 34-36.
5. Yu C, Meng X, Zhang S, Zhao G, Hu L, Kong X: A 3-nucleotide deletion in the polypyrimidine tract of intron 7 of the DFNA5 gene causes nonsyndromic hearing impairment in a Chinese family. *Genomics* 2003; **82**: 575-579.
6. Gregan J, Van Laer L, Lieto LD, Van Camp G, Kearsey SE: A yeast model for the study of human DFNA5, a gene mutated in nonsyndromic hearing impairment. *Biochim Biophys Acta* 2003; **1638**: 179-186.
7. Van Laer L, Vrijens K, Thys S *et al*: DFNA5: hearing impairment exon instead of hearing impairment gene? *J Med Genet* 2004; **41**: 401-406.
8. Van Laer L, Meyer NC, Malekpour M *et al*: A novel DFNA5 mutation does not cause hearing loss in an Iranian family. *Journal of Human Genetics* 2007; **52**: 549-552.
9. Van Laer L, Pfister M, Thys S *et al*: Mice lacking Dfna5 show a diverging number of cochlear fourth row outer hair cells. *Neurobiol Dis* 2005; **19**: 386-399.

- 1 10. Thompson DA, Weigel RJ: Characterization of a gene that is inversely correlated with  
2 estrogen receptor expression (ICERE-1) in breast carcinomas. *Eur J Biochem* 1998;  
3 **252**: 169-177.
- 4 11. Lage H, Helmbach H, Grottke C, Dietel M, Schadendorf D: DFNA5 (ICERE-1)  
5 contributes to acquired etoposide resistance in melanoma cells. *FEBS Lett* 2001; **494**:  
6 54-59.
- 7 12. Masuda Y, Futamura M, Kamino H *et al*: The potential role of DFNA5, a hearing  
8 impairment gene, in p53-mediated cellular response to DNA damage. *Journal of*  
9 *Human Genetics* 2006; **51**: 652-664.
- 10 13. Akino K, Toyota M, Suzuki H *et al*: Identification of DFNA5 as a target of epigenetic  
11 inactivation in gastric cancer. *Cancer Sci* 2007; **98**: 88-95.
- 12 14. Kim MS, Chang X, Yamashita K *et al*: Aberrant promoter methylation and tumor  
13 suppressive activity of the DFNA5 gene in colorectal carcinoma. *Oncogene* 2008; **27**:  
14 3624-3634.
- 15 15. Kim MS, Lebron C, Nagpal JK *et al*: Methylation of the DFNA5 increases risk of  
16 lymph node metastasis in human breast cancer. *Biochemical and Biophysical*  
17 *Research Communications* 2008; **370**: 38-43.
- 18 16. Fujikane T, Nishikawa N, Toyota M *et al*: Genomic screening for genes upregulated  
19 by demethylation revealed novel targets of epigenetic silencing in breast cancer.  
20 *Breast Cancer Res Treat* 2009.
- 21 17. Webb MS, Miller AL, Thompson EB: In CEM cells the autosomal deafness gene  
22 dfna5 is regulated by glucocorticoids and forskolin. *J Steroid Biochem Mol Biol* 2007;  
23 **107**: 15-21.
- 24 18. Subramanian A, Tamayo P, Mootha VK *et al*: Gene set enrichment analysis: a  
25 knowledge-based approach for interpreting genome-wide expression profiles.

- 1        *Proceedings of the National Academy of Sciences of the United States of America*  
2        2005; **102**: 15545-15550.
- 3    19.    Callebaut I, Labesse G, Durand P *et al*: Deciphering protein sequence information  
4        through hydrophobic cluster analysis (HCA): current status and perspectives. *Cell Mol*  
5        *Life Sci* 1997; **53**: 621-645.
- 6    20.    Eudes R, Le Tuan K, Delettre J, Mornon JP, Callebaut I: A generalized analysis of  
7        hydrophobic and loop clusters within globular protein sequences. *BMC Struct Biol*  
8        2007; **7**: 2.
- 9    21.    Gaboriaud C, Bissery V, Benchetrit T, Mornon JP: Hydrophobic cluster analysis: an  
10       efficient new way to compare and analyse amino acid sequences. *FEBS Lett* 1987;  
11       **224**: 149-155.
- 12   22.    Busch-Nentwich E, Sollner C, Roehl H, Nicolson T: The deafness gene *dfna5* is  
13       crucial for *ugdh* expression and HA production in the developing ear in zebrafish.  
14       *Development (Cambridge, England)* 2004; **131**: 943-951.
- 15   23.    Delmaghani S, del Castillo FJ, Michel V *et al*: Mutations in the gene encoding  
16       *pejvakin*, a newly identified protein of the afferent auditory pathway, cause DFNB59  
17       auditory neuropathy. *Nat Genet* 2006; **38**: 770-778.
- 18   24.    Tamura M, Tanaka S, Fujii T *et al*: Members of a novel gene family, *Gsdm*, are  
19       expressed exclusively in the epithelium of the skin and gastrointestinal tract in a  
20       highly tissue-specific manner. *Genomics* 2007; **89**: 618-629.
- 21   25.    Sha SH, Chen FQ, Schacht J: Activation of cell death pathways in the inner ear of the  
22       aging CBA/J mouse. *Hearing Research* 2009; **254**: 92-99.
- 23   26.    Walsh T, Pierce SB, Lenz DR *et al*: Genomic duplication and overexpression of  
24       *TJP2/ZO-2* leads to altered expression of apoptosis genes in progressive

1 nonsyndromic hearing loss DFNA51. *American Journal of Human Genetics*; **87**: 101-  
2 109.

3 27. Woodcock S, Mornon JP, Henrissat B: Detection of secondary structure elements in  
4 proteins by hydrophobic cluster analysis. *Protein Eng* 1992; **5**: 629-635.

5 **Titles and legends to figures**

6 **Figure 1:**

7 Panel A

8 Graphical representation of the insert content in relation to the construct's name. An exon is  
9 indicated by a rectangle containing the relevant exon number. The alternative reading frame  
10 used in the aberrant tail of mutant *DFNA5* is indicated with an asterisk.

11 Panel B

12 Western blot analysis of selected *DFNA5* constructs demonstrating that all constructs are  
13 expressed when transfected in HEK293T cells (using a pEGFP-N1 vector). Arrows point to  
14 the relevant position of the fusion proteins. Some degradation products are visible in lanes 2,  
15 3 and 5.

16 Panel C

17 Cell viability measurements 21 hours post transfection. Graphical bars represent the  
18 percentage of viable cells. An asterisk denotes statistically significant differences ( $p < 0.05$ )  
19 between transfections with the construct of interest and the WT construct. Control  
20 measurements are depicted in light gray colored bars, while constructs specific for this  
21 experiment are indicated with hatched bars. This series of transfections demonstrates that the  
22 toxic part of *DFNA5* is located in the first part of *DFNA5*. Interestingly, this indicates that the  
23 motif that is responsible for toxicity is shared by WT and mutant *DFNA5*.

24 Panel D

1 Subcellular localization of EGFP fusion proteins in HEK293T cells. Transfection of empty  
2 pEGFP-N1 vector results in an evenly distributed expression pattern throughout the cytosol.  
3 The first part of DFNA5 (exon 2 – exon 7) is localized mainly at the plasma membrane. Cell  
4 blebbing is seen in cells transfected with this construct. A similar pattern was observed when  
5 mutant *DFNA5* was transfected in HEK293T cells<sup>7</sup>. Both WT *DFNA5* exon 8 – exon 10 and  
6 WT *DFNA5* exon 9 – exon 10 are localized in the cytoplasm, near the nucleus. Cells  
7 transfected with the mutant *DFNA5* exon 9 - exon 10 construct, show expression in the  
8 endoplasmic reticulum (see also supplementary figure 1). A full color version of this figure  
9 can be found in the html version of this paper.

10 **Figure 2:**

11 HCA analysis of *DFNA5*, *GSDM1*, *MLZE* and *PJVK*. The sequences are shown on a  
12 duplicated  $\alpha$ -helical net, in which hydrophobic residues (VILFMYW) are contoured, forming  
13 clusters, which mainly correspond to the internal faces of regular secondary structures<sup>27</sup>. The  
14 way to read the sequences (1D) and secondary structures (2D) as well as special symbols are  
15 indicated in the inset. Conserved hydrophobic residues are shaded in grey, the vertical lines  
16 indicating the correspondences between the different sequences. Noticeable  
17 identities/similarities outside the hydrophobic clusters are encircled in grey. The predicted  
18 globular domains (A and B) are depicted with arrows. A hinge of variable length (grey box)  
19 separates domain A from domain B. Predicted secondary structures of these globular domains  
20 are indicated at the top. Domain B does not exist in *PJVK*, in which it is replaced by a shorter  
21 domain (contoured in grey), likely containing a zinc finger. A full color version of this figure  
22 can be found in the html version of this paper.

23 **Figure 3:**

24 Panel A

1 Confocal images of annexin V-Cy5-stained cell transfections. Cells transfected with WT  
2 *DFNA5* are negative for PI and annexin V-Cy5. Cells transfected with mutant *DFNA5* are  
3 negative for PI but show clear annexin V at the plasma membrane, which is suggestive for  
4 apoptotic cell death. All cells were harvested 16 hours post transfection. A full color version of  
5 this figure can be found in the html version of this paper.

6 Panel B

7 Flow cytometric quantification of annexin V-Cy5-stained transfected cells. Cells were  
8 harvested 16 hours post transfection. Percentages of apoptotic cells within the total cell  
9 population are shown. The total apoptotic fraction was calculated as the sum of the early  
10 (annexin V+ PI-) and late (annexin V+ PI+) apoptotic fractions.

11 **Figure 4:**

12 Panel A

13 Confocal images of WT *DFNA5* (left pane of image)- versus mutant *DFNA5* (right pane of  
14 image)-transfected HEK293T cells, stained with the in situ cell death detection kit, TM Red.  
15 TUNEL-positive cells show bright staining of the nucleus. A full color version of this figure  
16 can be found in the html version of this paper.

17 Panel B

18 Quantitative measurement of TUNEL-positive cells relative to the total cell population. Cells  
19 transfected with mutant *DFNA5* show significantly more apoptosis compared to controls. All  
20 cells were harvested 16 hours post transfection.

**a**

WT DFNA5 exon 2 - exon 7



WT DFNA5 exon 8 - exon 10



WT DFNA5 exon 9 - exon 10



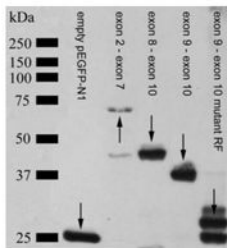
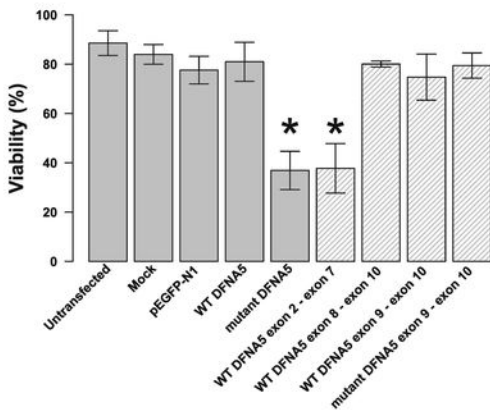
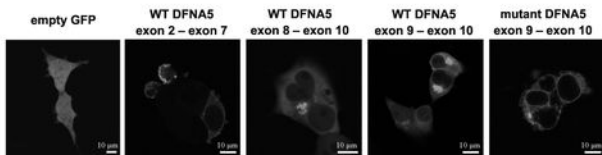
mutant DFNA5 exon 9 - exon 10



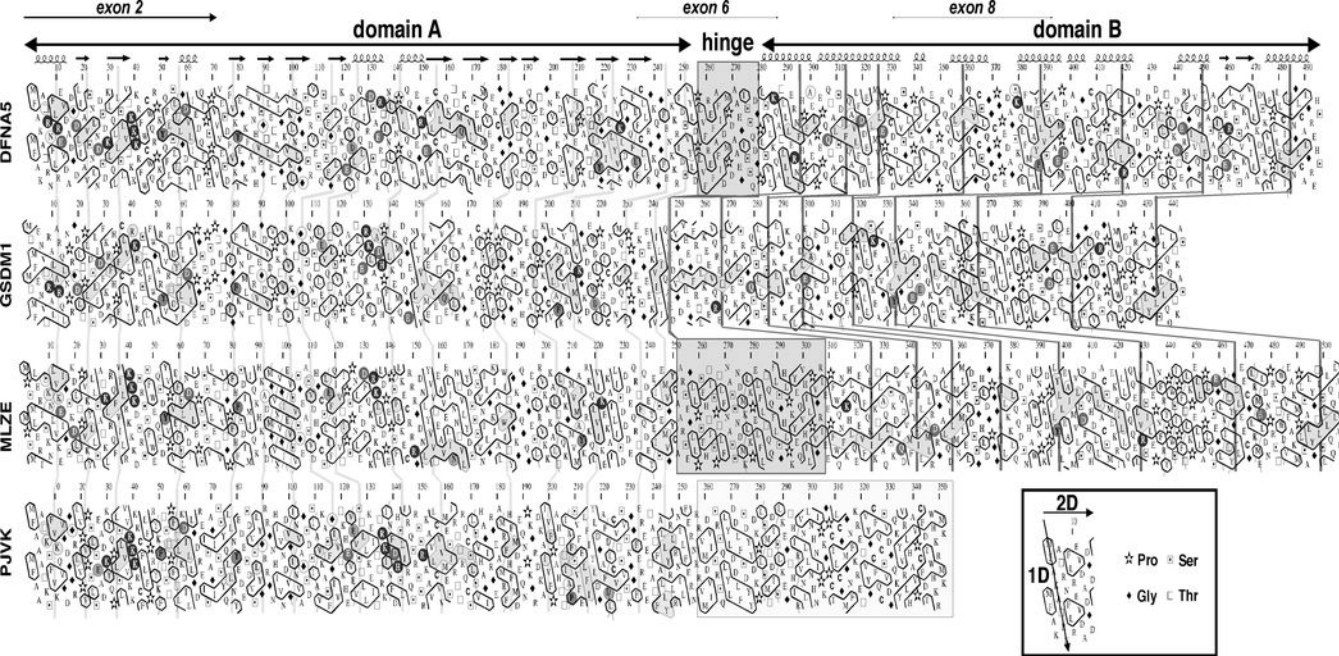
WT DFNA5



mutant DFNA5

**b****c****d**

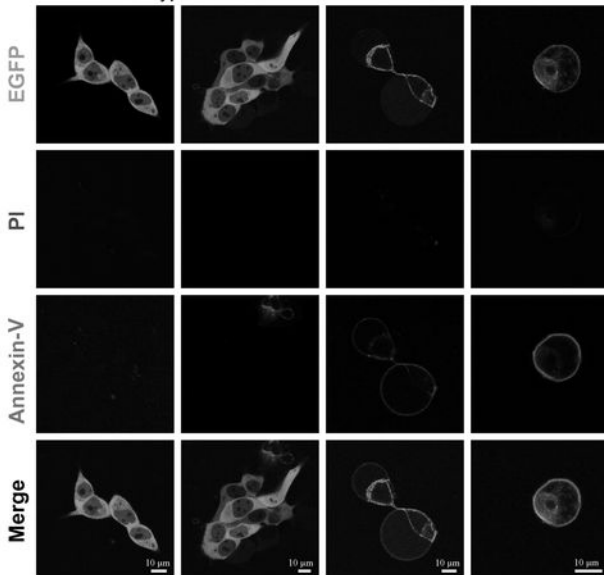
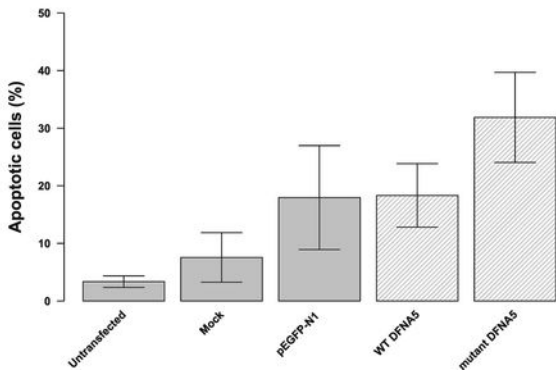




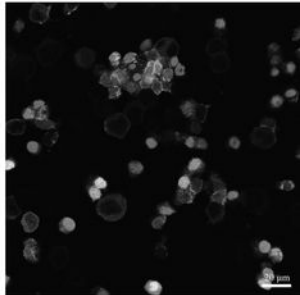
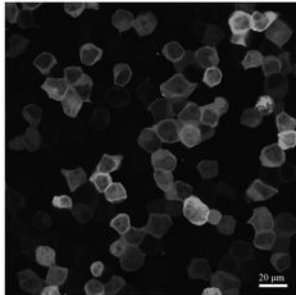
**a**

Wild Type DFNA5

Mutant DFNA5

**b**

a



b

